Published in final edited form as:
Neurochem Int. 2013 January ; 62(2): 145–156. doi:10.1016/j.neuint.2012.12.001.

Alzheimer Disease Periventricular White Matter Lesions Exhibit Specific Proteomic Profile Alterations

Eduardo M. Castaño[1,*], **Chera L. Maarouf**[2], **Terence Wu**[3], **Maria Celeste Leal**[1], **Charisse M. Whiteside**[2], **Lih-Fen Lue**[4], **Tyler A. Kokjohn**[5], **Marwan N. Sabbagh**[6], **Thomas G. Beach**[7], and **Alex E. Roher**[2,*]

[1]Fundación Instituto Leloir and Instituto de Investigaciones Bioquímicas de Buenos Aires, Consejo Nacional de Investigaciones Científicas y Técnicas (CONICET), Patricias Argentinas 435, Buenos Aires C1405BWE, Argentina

[2]The Longtine Center for Neurodegenerative Biochemistry, Banner Sun Health Research Institute, 10515 W. Santa Fe Dr., Sun City, AZ 85351, USA

[3]The W.M. Keck Laboratory, Yale University, 300 George Street, Box 201, New Haven, CT 06511, USA

[4]Laboratory of Neuroregeneration, Banner Sun Health Research Institute, 10515 West Santa Fe Drive, Sun City, AZ 85351, USA

[5]Department of Microbiology, Midwestern University School of Medicine, 19389 N. 59th Ave., Glendale, AZ 85308, USA

[6]Roberts Clinical Center, Banner Sun Health Research Institute, 10515 W. Santa Fe Dr., Sun City, AZ 85351, USA

[7]Harold Civin Laboratory of Neuropathology, Banner Sun Health Research Institute, 10515 W. Santa Fe Dr., Sun City, AZ 85351 USA

Abstract

The white matter (WM) represents approximately half the cerebrum volume and is profoundly affected in Alzheimer's disease (AD). However, both the WM responses to AD as well as potential influences of this compartment to dementia pathogenesis remain comparatively neglected. Neuroimaging studies have revealed WM alterations are commonly associated with AD and renewed interest in examining the pathologic basis and importance of these changes.

In AD subjects, immunohistochemistry and electron microscopy revealed changes in astrocyte morphology and myelin loss as well as up to 30% axonal loss in areas of WM rarefaction when measured against non-demented control (NDC) tissue. Comparative proteomic analyses were performed on pooled samples of periventricular WM (PVWM) obtained from AD (n = 4) and NDC (n = 5) subjects with both groups having a mean age of death of 86 years. All subjects had an apolipoprotein E ε3/3 genotype with the exception of one NDC subject who was ε2/3. Urea-

[*]**Corresponding Authors:** Eduardo M. Castaño, MD., Fundación Instituto Leloir and Instituto de Investigaciones Bioquímicas de Buenos Aires, Consejo Nacional de Investigaciones Científicas y Técnicas (CONICET), Patricias Argentinas 435, Buenos Aires C1405BWE, Argentina, Phone: (54-11) 5238-7500 (ext 3104), Fax: (54-11) 5238-7501, ecastano@leloir.org.ar; Alex E. Roher, MD., PhD., Longtine Center for Neurodegenerative Biochemistry, Banner Sun Health Research Institute, 10515 W. Santa Fe Dr., Sun City AZ, 85351, Phone: 623-832-5465, Fax: 623-832-5698, alex.roher@bannerhealth.com.

detergent homogenates were analyzed using two different separation techniques: 2-dimensional isoelectric focusing/reverse-phase chromatography and 2-dimensional difference gel electrophoresis (2D-DIGE). Proteins with different expression levels between the 2 diagnostic groups were identified using MALDI-Tof/Tof mass spectrometry. In addition, Western blots were used to quantify proteins of interest in individual AD and NDC cases.

Our proteomic studies revealed that when WM protein pools were loaded at equal amounts of total protein for comparative analyses, there were quantitative differences between the 2 groups. Molecules related to cytoskeleton maintenance, calcium metabolism and cellular survival such as glial fibrillary acidic protein, vimentin, tropomyosin, collapsin response mediator protein-2, calmodulin, S100-P, annexin A1, α-internexin, α-and β-synuclein, α-B-crystalline, fascin-1, ubiquitin carboxyl-terminal esterase and thymosine were altered between AD and NDC pools.

Our experiments suggest that WM activities become globally impaired during the course of AD with significant morphological, biochemical and functional consequential implications for gray matter function and cognitive deficits. These observations may endorse the hypothesis that WM dysfunction is not only a consequence of AD pathology, but that it may precipitate and/or potentiate AD dementia.

Keywords

Alzheimer's disease; periventricular white matter; white matter rarefaction; proteomics; glial fibrillary acidic protein; axonal loss; myelin loss

1. Introduction

Alzheimer's disease (AD) is neuropathologically defined by the presence of neurofibrillary tangles (NFT), amyloid plaques (AP) and cerebral amyloid angiopathy (CAA) mainly observed in neocortical and allocortical gray matter (GM). In addition, gross abnormalities in the white matter (WM), recognized as WM hyperintensities (WMH) by magnetic resonance imaging (MRI), lucencies on computed tomography scans or neuropathologically defined as WM rarefaction (WMR), are detected in approximately two/thirds of the patients with confirmed AD. These abnormalities include partial loss of myelin, degeneration of axons and oligodendrocytes, reactive astrocytosis, microglial activation with the presence of macrophages, hyaline fibrosis of small vessels, loss of microvessels, interstitial fluid stasis and chronic inflammation (Brun and Englund, 1986; Englund and Brun, 1990; Scheltens et al., 1995; Kalaria, 2002; Bronge et al., 2002; Roher et al., 2003b; Sjobeck et al., 2006; Kalback et al., 2004; Beach et al., 1989; Hachinski et al., 1987). WMH have also been found to correlate with increased Braak staging and neuritic plaque core densities in AD subjects (Polvikoski et al., 2010). In areas of white matter pathology (WMP), total cell and blood vessel counts exhibit strong inverse correlations with the mini-mental state examination, NFT score and Braak stage (Kalback et al., 2004). Using several biochemical methods, our group demonstrated that AD WM harbors significantly increased quantities of Aβ40 and Aβ42 accompanied by statistically significant decreases in the amounts of cholesterol, fatty acids, myelin basic protein, myelin proteolipid protein, and 2′, 3′-cyclic nucleotide 3′-phosphodiesterase compared with NDC subjects (Roher et al., 2002). WMP can be a pervasive process that correlates with a dramatic decline in cognitive functions (Duan et al., 2006).

Increasingly sophisticated neuroimaging studies have renewed interest in AD WMP. Techniques such as diffusion tensor imaging (DTI) have been used to characterize WMP in terms of tissue integrity, localization and functionality. DTI allows for a three-dimensional description of both the direction and the average magnitude of water diffusion, which is

more anisotropic in the highly organized WM than in the GM. DTI measures of WM anisotropy such as fractional anisotropy are widely used as markers of WM integrity (Pierpaoli and Basser, 1996; Beaulieu, 2002; Bozzali et al., 2002; Medina and Gaviria, 2008). In AD, fractional anisotropy reductions have been described in a variety of WM regions including the posterior corpus callosum, posterior cingulum, fornix, uncinate, commissural and parahippocampal fibers (reviewed by Zhang et al (2009)). Some of these lesions isolate the hippocampus from neocortical input impairing learning and declarative memory (Salat et al., 2010). Moreover, WM anisotropy in late myelination pathways such as the posterior cingulum bundles correlates with declining declarative memory in patients with mild cognitive impairment (MCI), of which 10-15% per year are known to progress to AD (Fellgiebel et al., 2005; Rose et al., 2006). Postmortem quantitative MRI and neuropathological correlation showed that axonal density was an independent determinant of fractional anisotropy, whereas T-1 relaxation time was independently determined by axonal and myelin density and microglial activation (Gouw et al., 2008). Semiquantitative and automated volumetric studies of WMH using MRI suggest that periventricular WM (PVWM) damage correlates better with cognitive decline than deep WMH (van Straaten et al., 2008). A possible explanation is the compromise of long association tracts connecting more distant cortical regions and the involvement of cholinergic pathways (Selden et al., 1998).

Two major mechanisms may account for the WMP in AD: 1) anterograde degeneration of axons originating in cortical areas with AP and NFT and 2) a primary compromise of WM due to multiple causes, including oligemia/hypoperfusion, microinfarcts (Suter et al., 2002), microvascular hypertensive disease, oxidative stress, myelin degeneration, traumatic brain injury and leukoencephalopathies (Al-Hasani and Smith, 2011). *In vivo* imaging has generated data in support for both possibilities (O'Dwyer et al., 2011b).

Multiple indices of diffusion in non-demented control (NDC), MCI (with or without amnesia) and AD subjects demonstrated that late myelination pathways are particularly affected in MCI and AD (O'Dwyer et al., 2011a). These results strengthen the "retrogenesis" hypothesis which proposes that in AD WM degeneration proceeds in a sequence that is the reverse of ontogenic myelinization in the CNS (Stricker et al., 2009; Bartzokis, 2004; Bartzokis, 2011; Braak and Del Tredici, 2004; Choi et al., 2005; Reisberg et al., 1992). The retrogenesis concept supports the possibility that AD pathogenesis may commence in the WM, rather than in the GM, with oligodendrocyte dysfunction that results in lack of axonal support leading to loss of myelin and alterations in the axonal cytoskeleton (Braak and Braak, 1996).

To better understand the biochemical cascades that underlie the complex anatomo-pathological and imaging features exhibited in the WM of AD patients, we performed a comparative sub-proteomic analysis of the PVWM of AD and NDC cases. The PVWM fractions examined in our current study contained only molecules which were soluble in urea-detergent containing buffers. We utilized two different separation techniques: PF2D liquid chromatography and 2-dimensional difference gel electrophoresis (2D-DIGE). In addition, immunohistochemistry, electron microscopy and Western blot analyses were used to examine WM changes that occurred in AD relative to those observed in NDC individuals. Our findings complement and expand previous pathological reports concerning astrogliosis, axonal damage, demyelination and microglial activation and emphasize the enormous critical, direct role of WM in the pathogenesis and development of dementia. The identification of several differentially expressed proteins provides more insights into the possible mechanisms that participate in the multifactorial and chronic WM damage in AD.

2. Material and Methods

2.1. Study Subjects

The subjects (AD = 4; NDC = 5) were selected from the Brain and Body Donation Program at Banner Sun Health Research Institute (Beach et al., 2008). The relatively small sample size is due, in part, to the stringent selection of individuals with extensive WMR of the periventricular areas and with the diagnosis of pure and uncomplicated AD, free of other simultaneous co-morbidities such as dementia with Lewy bodies, progressive supranuclear palsy, frontotemporal lobar degeneration, parkinsonism, etc. In addition, our NDC subjects do not have any of the common neurodegenerative disorders that affect the elderly population and do not have the neuropathological hallmarks of AD (Table 1) including evidence of WMR. Furthermore, we selected individuals with low postmortem intervals (mean 2.8 h and 2.7 h, for the NDC and AD groups, respectively) to minimize postmortem lysis. Likewise, the individuals were selected to match their ages (mean 86 years for both cohorts). Table 1 shows the demographics and neuropathology of the AD and NDC subjects. The mean brain weight of the NDC cohort was 1112 g and 1070 g for the AD group. All subjects carried the apolipoprotein (ApoE) ε3/3 genotype, except for the NDC patient #5 which was an ApoE ε2/3. Forty μm thick coronal sections were stained with Campbell-Switzer, Thioflavine-S, Gallyas and hematoxylin and eosin (H&E) to assess AP, NFT, CAA and WMR. The occurrence of dementia and an NIA-Reagan rating of at least “intermediate” in terms of neuritic plaque density and Braak NFT stage was used to determine the clinicopathological diagnosis of AD (National Institute on Aging, 1997). Neuropathological scoring included total plaque score (max. 15), total NFT score (max. 15), Braak stage (range I-VI), total CAA score (max. 12) and total WMR score (max. 12). A detailed description of the neuropathological scoring procedures is given elsewhere (Beach et al., 2008; Maarouf et al., 2011; Roher et al., 2003a).

2.2. Immunohistochemistry

Coronal sections of 40 μm thickness from the frontal lobe were washed in phosphate buffered saline (PBS) containing 0.3% Triton-X100 (PBS-T) 3 times to remove the storage buffer. The sections were placed into rabbit anti-glial fibrillary acidic protein (GFAP, DAKO, Carpinteria, CA, catalog #Z0334) at a dilution of 1:3000 and incubated at room temperature (RT) for 20 h on an orbital shaker. The sections were removed from primary antibody washed 6 times, 5 min each, in PBS-T and placed in Alexa Fluor 488-conjugated goat anti-rabbit IgG antibody (Life Technology Corp., Carlsbad, CA, catalog #A-11034) at 1:1000 dilution for 2 h at RT on an orbital shaker. After washing (6 times, 5 min each in PBS-T) the sections were mounted onto glass plus slides and dried. The slides were placed into 70% ethanol for 5 min, 1% Sudan black in 70% ethanol for 2 min, 50% ethanol for 5 min, rinsed in dH_2O and then cover slipped using Vectashield mounting media (Vector Labs, Burlingame, CA).

2.3. Tissue samples

A pool of PVWM from 4 AD (250 mg each) and 5 NDC (200 mg each) subjects was homogenized at 4°C in 20 ml of Beckman’s Proteome Lab Start Buffer which contains a proprietary mix of urea, n-octylglucoside, triethanolamine and is adjusted to pH 8.5 with iminodiacetic acid. The samples were centrifuged for 2 h at 280,000 x g with a Beckman SW41 rotor at 4°C. The supernatant was collected and saved at −80°C for analysis in the Beckman PF2D liquid chromatographic system.

2.4. 2D-DIGE

The insoluble pellets were suspended in 7 M urea, 2 M thiourea, 4% CHAPS, 25 mM Tris-HCl, pH 8.5. Fifty μg of the NDC proteins and 50 μg of the AD proteins were labeled with Cy-3 and Cy-5 N-hydroxysuccinimidyl ester dyes, respectively. The proteins were first separated by isoelectric focusing using pH 3-10 IPG strips and then by SDS gel electrophoresis using 12.5% polyacrylamide gels. The gels were stained with Sypro Ruby and scanned with different wavelengths on a GE Healthcare Typhoon 9410 Imager. Quantitative analysis was performed with GE Healthcare DeCyder software to discover the proteins that had different expression levels. Spots with at least 2-fold differences between AD and NDC were robotically picked and digested with trypsin. Protein identification was performed on an Applied Biosystems 4800 MALDI-Tof/Tof mass spectrometer and the data analyzed by the Applied Biosystems GPS Explorer software. Mascot analysis against the NCBInr database and a combined peptide mass fingerprint/MS/MS search was run. Only proteins with significant Mascot scores of 80 or greater were included.

2.5. PF2D chromatography

Proteins were fractionated by their pI and then in the second dimension by their hydrophobicity using a reverse phase column. The AD and NDC PVWM pools were run with a ProteomeLab™ PF2D chemistry kit (Beckman Coulter, Fullerton, CA) following the manufacturers protocols as well as detailed protocols that have been published elsewhere (Linke et al., 2006; Ruelle et al., 2007). A total of 4 mg of protein for each diagnostic pool was brought to 5 ml with Start Buffer and was injected into the first dimension chromatofocusing column. A linear pH gradient was created in the column using the Start Buffer (pH 8.5) and Eluent Buffer (pH 4.0) at a flow rate of 0.2 ml/min and fractions were automatically collected every 0.3 pH units. After the protein gradient was completed, a high salt wash (1 M NaCl) and then a water wash were passed through the column. Proteins eluting above pH 8.5 and below pH 4.0 were collected every 5 min. The fractions were collected in a 96-well plate inside a cooled collector/injector that is connected to the second dimension. The fractions collected in the first dimension were submitted to a C18 reverse phase column kept at 50°C using a linear gradient generated from 0.1% (v/v) trifluoroacetic acid (TFA, Sigma, St. Louis, MO) in HPLC grade water (Aristar, VWR, West Chester, PA) to 0.08% TFA in acetonitrile (JT Baker, Phillipsburg, NJ) at a flow rate of 0.75 ml/min over 45 min. Fractions were collected every 0.4 min in 96-well plates using a Gilson FC204 fraction collector between 10 and 22 min and stored at −80°C. Data analysis was performed on the second dimension results with DeltaVue software (Beckman) which allows side-by-side comparison of two different samples. Proteins from differential peaks between AD and NDC samples were identified after trypsin digestion and mass spectrometry as described above.

2.6. Western blot analysis

One-hundred mg of PVWM from each case in Table 1 was homogenized in 1000 μl of 5% SDS, 5 mM EDTA, 20 mM Tris-HCl, pH 7.8 with an electric tissue grinder (Omni TH, Kennesaw, GA). The supernatant was collected after centrifugation at 14,000 x g for 20 min in a Beckman 22R centrifuge and total protein quantified with Pierce's Micro BCA protein assay kit (Rockford, IL). Ten or 40 μg of total protein was reconstituted in NuPage 2XLDS sample buffer (Life Technologies Corp.), 50 mM dithiothreitol (Sigma, St. Louis, MO) and heated for 10 min at 80°C. Protein separation was performed on 10 well 4-12% Bis-Tris gels with NuPage 1XMES SDS running buffer with NuPage antioxidant (Life Technology Corp.). The prestained Kaleidoscope marker (Bio-Rad, Hercules, CA) was used as a molecular weight standard. After protein transfer onto 0.45 μm nitrocellulose membranes (Life Technology Corp.) with NuPage transfer buffer (Life Technology Corp.) and 20% methanol (Pharmco-Aaper), the membranes were blocked in 5% Quick-Blocker (G-

Biosciences, Maryland Heights, MO) in PBS (EMD Chemicals, Gibbstown, NJ), 0.5% Tween20. All antibodies were diluted in blocking buffer. The primary and secondary antibodies employed in these Western blots are described in supp. Table I. Proteins were detected with SuperSignal WestPico Chemiluminescent (Pierce) substrate on CL-Xpose film (Pierce) with Kodak GBX developer and fixer. All membranes were stripped with Restore™ Western Blot Stripping Buffer (Pierce), washed, re-blocked and re-probed with anti-mouse actin (BD Transduction Laboratories) or anti-rabbit actin antibody (Abcam). A GS-800 calibrated densitometer (Bio-Rad) and Quantity One software (Bio-Rad) were employed for densitometry analysis and the units reported in optical density (OD) x mm.

3. Results

On average, the AD cohort had 6.4-fold and 4.2-fold higher total plaque scores and total NFT scores than the NDC subjects, respectively (Table 1). The Braak stage was more advanced in the AD cases (Table 1). The NDC group did not have observable CAA while the AD individuals had a mean total CAA score of 2 (Table 1). The WMR score was employed to select specific contrasting case groups for this study. The NDC cases exhibited no discernable WMR while the AD cases examined all possessed severe WMR (Table 1). A representative coronal section stained with H&E from each diagnostic group is shown in Figures 1A and 1B. The lighter-stained areas represent WMR and the boxed areas delineate the PVWM used in the experimental analyses (Figure 1A and 1B). Astrocytes were visualized in the deep WM using an antibody against GFAP (Figure 1C and 1D). The morphology of the astrocytes in an NDC subject (case #4) revealed stellar bodies, fine ramified fibrous processes and smooth surfaces that extended over long distances (Figure 1C). In contrast, the astrocytes in the deep WM from AD case #13 showed astrocytic bodies that resemble the protoplasmic type with shorter processes of variable caliber and an abundance of granular positive GFAP (Figure 1D). These observations may correlate with dilated astrocytic cell processes (see Figure 2). Electron microscopy depicts the loss of cells and severe demise of axons and myelin in an AD subject with severe WMR relative to a NDC subject without WMR (Figures 2A and 2B).

To obtain comprehensive 2D proteomic analytical patterns, we specifically selected extraction strategies based on protein solubility that were compatible with the two proteomic separation techniques. After ultracentrifugation, the urea/n-octylglucoside soluble fraction was analyzed by PF2D liquid chromatography. The remaining pellet was re-homogenized in urea/thiourea/CHAPS, centrifuged and the supernatant submitted to 2D-DIGE.

Separation of the insoluble pellet by 2D-DIGE yielded 27 spots with a >2-fold difference between NDC (Figure 3A) and AD (Figure 3B) pools. Their identities are listed in Table 2. Twenty-three spots were ultimately identified as GFAP. In the 2D-DIGE gels, a major field of molecular differences between NDC and AD clustered between 35-50 kDa and pH 4-6 (Figure 3C), a profile consistent with a previous 2D gel report (Korolainen et al., 2005). The same study found a 60% increase in AD brains of phosphorylated or N-glycosylated acidic isoforms of GFAP (Korolainen et al., 2005). In addition, we identified 3 spots of about 75-80 kDa (spot #1-3) corresponding to SDS-resistant GFAP aggregates (Figure 3C). As revealed by the presence of tryptic peptides corresponding to residues 320-330, these are probably dimeric truncated GFAP forms that conserve the rod domain. These high molecular-weight GFAP species were elevated 2-fold in the AD pool. Interestingly, the highest quantitative differences (~6 to 8-fold increase in AD) were found in a ~38-40 kDa acidic protein spot cluster corresponding to spot #21-26 (Figure 3C and Table 2). Taking as a reference the 432-residue canonical GFAP-α isoform, the identification of tryptic peptides from position 96 to position 367 suggests these are amino and carboxyl-terminally truncated GFAP. Similar GFAP isoforms analyzed in a prior paper did not show major differences

between AD and NDC subjects. However, the samples analyzed were from the frontal cortex (Korolainen et al., 2005) and relatively more soluble than those from PVWM used in the present study. Although the GFAP identified by 2D-DIGE was likely the most common isoform1 (α), no peptides were identified by this method beyond position 390, after which amino acid sequences differ between GFAP-α and GFAP-Δ/ε. Due to this limitation, we cannot rule out a contribution of these rare isoforms to some of the differences observed (Nielsen et al., 2002). Two spots (#4 and #6) at ~50 kDa and ~pI 5, with a 2-fold increase in the AD group, yielded peptides derived from vimentin (VIM), likely corresponding to the full-length protein (Figure 3C and Table 2). One spot at ~35 kDa and pI 7 with a 2.2-fold increase was identified as annexin A1 (ANXA1) and one spot at ~50 kDa, pI 7 was identified as fascin-1 (FSCN1) showing a 2.2.-fold reduction in AD samples compared to NDC (Figure 3C and Table 2).

Proteins in the supernatant were separated by PF2D liquid chromatography with a first dimension based on pI using a pH 4-8.5 gradient, followed by a second dimension partition utilizing hydrophobic exchange. Because numerous tryptic peptides from different proteins were expected in each peak due to the high sensitivity of the method, we applied stringent selection criteria to unambiguously identify differentially expressed proteins after chromatographic detection: 1) total peak absorbance ~0.1; 2) the presence of the same protein in at least two different peaks with absorbance ~0.1; 3) the same tendency (higher or lower absorbance in AD compared to NDC) in all the peaks in which the protein was found; 4) more than one peptide identified for each protein and 5) a MASCOT database score cutoff of 82.

Of a total of 89 protein peaks, 4 peaks (I, II, III and V) had ODs between 0.1 to 0.6 and showed a ~4 to 7-fold increase in AD as compared to NDC pools (Figure 4A-C and Tables 3, 4 and 6). Only one fraction (peak IV) with OD ~0.1 was highly increased (~10-fold) in the NDC as compared to the AD group (Figure 4C and Table 5). These five fractions were selected for protein identification by trypsin digestion and mass spectrometry. The complete list of proteins identified in each of these peaks is shown in Tables 3-6. GFAP-α was identified in all peaks (Tables 3-6) while VIM, tropomyosins (TPMs), calmodulin (CALM), α-internexin (INA) and β-synuclein were found in two fractions with the highest ODs (Figure 4B and Table 4), suggesting that these proteins were increased in the PVWM of AD subjects as compared with NDC individuals. The extent of primary amino acid sequence coverage by the identified tryptic peptides, which was greater than 90% for GFAP-α and greater than 68% for VIM and CALM (Table 4), or the identification of peptides from amino and carboxy-terminal regions in the case of INA (a 500-aa protein), suggested that these proteins were not fragmented extensively during the extraction and chromatographic procedures. Proteins identified in fraction IV with elevated NDC absorbance included thymosine (TMS)-β4, GFAP, collapsin response mediator protein-2 (CRMP-2), myelin basic protein and α-B-crystallin (Table 5 and Figure 4C). Two additional isoforms of TMS were increased in the AD pool of fraction V (Table 6 and Figure 4C).

Well-characterized, commercially available antibodies for GFAP, VIM, ANXA1, FSCN1, INA and TPM3 (Suppl. Table I) were used to further characterize these molecules by Western blots. Quantitative analysis showed individual variability within groups which was more notorious in AD cases (Figure 5). Both mean GFAP and VIM levels were increased in the AD group by 20% (Figure 5A) and 45% (Figure 5B), respectively, when compared to the NDC subjects. Mean quantities of ANXA1 showed a 2.4-fold increase (Figure 5C) while FSCN1 was reduced 19% (Figure 5D) in the AD group compared to the NDC subjects, consistent with the results obtained by 2D-DIGE. On the average, INA was increased ~9% (Figure 5E) while TPM3 was decreased by 18%, in AD as compared with NDC individuals

showing the same trend as in PF2D chromatography but without reaching statistical significance.

The concurrent results of at least two out of three independent analytical methods indicate that GFAP, VIM and ANXA1 are over-expressed while FSCN1 was reduced in the PVWM of AD individuals. INA was also observed to be increased in AD by PF2D and Western blots. The only proteins found to be higher in NDC subjects were those in fraction IV (see Figure 4C and Table 5). This increase was remarkable (10-fold) and some of the proteins involved have been related in several ways with AD pathogenesis. However, caution must be applied when comparing and interpreting results from different separative and quantitative technologies. For example, the polyclonal anti-GFAP antibody used in Western blots was raised against a recombinant DNA engineered amino acid sequence and does not show the many post-translational modifications that occur in this protein. On the other hand, the proteomic maps (ideally) give an account of multiple isoforms that exist under healthy or deviate under pathological conditions, which include N- and C-terminal degradations and a flurry of post-translationally modifications at different sites with different rates of occurrence.

4. Discussion

Despite the fact that the WM represents 50% of the cerebrum and that WM tissues become substantially atrophied and profoundly abnormal in AD (Brunetti et al., 2000; Smith et al., 2000; DeCarli et al., 1996; Kawamura et al., 1992), there is a paucity of information regarding WM biochemical alterations and their contribution to the pathogenesis of this dementia. A query of the PubMed database using combined search terms of “proteomics, white matter, Alzheimer’s disease” confirmed the lack of investigations in this general area.

Electron microscopy studies of AD patient WM demonstrate widespread loss of axons and myelin in areas of WMR that are replaced with an extensive network of hypertrophic astrocytes. Although we did not find a strong difference in the overall amount of GFAP, as detected by Western blot, there are clear qualitative alterations in many of the isoforms of this molecule between AD and NDC PVWM pools as assessed by two different proteomic techniques. A large number of molecular mediators of astrogliosis associated with aging and neurodegenerative disorders (Sofroniew, 2009) have been identified including growth factors, cytokines, Aβ peptides, hypoxia related molecules, reactive oxygen species and glutamate. In AD, increased GFAP immunoreactivity has been found consistently in astrocytes surrounding neuritic plaques and blood vessels (Duffy et al., 1980; Schechter et al., 1981; Mancardi et al., 1983; Beach et al., 1989; Muramori et al., 1998). Furthermore, it has been suggested that the levels of GFAP in several cortical regions correlate inversely with cognitive performance (Kashon et al., 2004) and this molecule is elevated in the cerebrospinal fluid of demented patients (AD and non-AD) as compared to controls (Jesse et al., 2009; Wallin et al., 1996). Interestingly, an early work showed a strong increase of GFAP in brain regions with few or no typical AD lesions (such as cerebellum, striatum and brain stem) similar to our findings, demonstrating that PVWM astrocyte reaction does not depend on Aβ and/or tau aggregate physical proximity (Delacourte, 1990).

Interestingly, GFAP toxicity may be mitigated by the small heat shock protein α-B-crystallin (Tang et al., 2010; Hagemann et al., 2009), which exhibited a net reduction in AD PVWM in our PF2D proteomic analysis. Alpha-B-crystallin is a molecule of the family of heath shock proteins that may have important neuroprotective activities in AD (reviewed by Smith et al (2005)), and act as chaperones that prevents protein aggregation (Ecroyd and Carver, 2009). Increased GFAP levels coupled with reduced α-B-crystallin suggest a possible pathogenic loop promoting GFAP toxicity in the WM.

The concurrent overexpression of GFAP and VIM in WMP is suggestive of diffuse reactive astrocytosis associated with pronounced hypertrophy of cell body and processes, disruption of individual astrocytic domains and proliferation and migration into sites of injury (Petito et al., 1990; Wang et al., 2004). WM reactive astrogliosis may contribute to the AD neurodegenerative process by inhibiting axonal regeneration (Wilhelmsson et al., 2004; Toyooka et al., 2011).

The up-regulation of ANXA1 in AD WMP which we found by 2D-DIGE and Western blot, is concurrent with the activation of microglial cells in the WM of AD patients (Gouw et al., 2008). ANXA1 overexpression may indicate an attempt to limit sustained inflammatory damage due to unknown factors in AD WM. Fibrillar Aβ deposits are capable of activating microglia (Jana et al., 2008) and it remains to be tested whether non-fibrillar Aβ, at the levels found in AD WM, which are ~4-fold of those observed in NDC subjects (Roher et al., 2002), are capable of promoting ANXA1 expression.

Our 2D-DIGE and Western blot analysis revealed a decrease in FSCN1 in the AD pool relative to the NDC pool. FSCN1 is present in neurons, glia and endothelial cells and promotes F-actin assembly into ordered bundles in the cytoplasm and cell protrusions contributing to cell adhesion and migration (reviewed by Adams (2004)). Interestingly, FSCN1 interacts with voltage-dependent anion channel 1 (VDAC1) (Ewing et al., 2007), a mediator of endothelial cell apoptosis triggered by endostatin which in turn binds to Aβ42 (Yuan et al., 2008; Faye et al., 2009). Since vascular depletion is a major and pathogenically relevant feature in AD WMP (Kalback et al., 2004), FSCN1 reduction may also affect endothelial survival adversely.

Our proteomic analysis of the soluble fraction of the PVWM found that two molecules potentially affecting cytoskeleton organization and activities were altered in AD. TMP3 is elevated in the hippocampus of AD brains (Owen et al., 2009). In vitro studies have shown that TMPs enhance the pointed-end capping activity of tropomodulins on actin microfilaments and that TMP3 overexpression in primary neurons is capable of inhibiting neurite outgrowth (Fath et al., 2011; Schevzov et al., 2005). Together, the reduction of FSCN1 and the accumulation of TPM3 in the WMP of AD may have profound deleterious effects on the dynamics of actin cytoskeleton organization. The decrease of CRMP-2 in AD relative to NDC subjects suggests disturbances in the extension and retraction of cell processes in neurons and oligodendrocytes which are critical for cell migration, axonal contact and myelination (Dawson et al., 2003). In neurons, phosphorylation of CRMP-2 assists in microtubule disassembly (Arimura et al., 2005; Uchida et al., 2005). We have recently shown that phosphorylation of CRMP-2 promotes retraction of oligodendrocyte processes in response to non-lethal oxidative stress (Fernandez-Gamba et al., 2012).

The peptide TMS-β4 was identified in both peaks IV and V with opposite quantitative trends. TMS-β4 is differentially acetylated and phosphorylated at several Lys and Thr residues (Hannappel, 2010) and these differences may reflect post-translational modifications that result in different isoelectric points. TMS-β4 is a multifunctional peptide that promotes stem cell differentiation, cell migration, cell survival and angiogenesis and intervenes in tissue regeneration and repair (Crockford et al., 2010).

The Ca2+ binding proteins S100P and CALM were also increased in AD PVWM. It is possible that increases in S100P are an attempt to enhance cell proliferation (Arumugam et al., 2004), while CALM up-regulation may be an effort to maintain multiple metabolic cascades, including signal transduction, essential for cell survival (Chin and Means, 2000).

Elevated quantities of ubiquitin carboxy-terminal esterase L1, as shown in the PF2D analysis, may be involved in the degradation of excessive Aβ via the proteosome system

(Gong et al., 2006). In addition, our proteomic analysis also revealed that α- and β-synuclein are accumulated in the AD PVWM. Although the precise functions of these molecules have not been defined it was recently found that α-synuclein is also often elevated in AD (Larson et al., 2012).

Our proteomic examination of PVWM shows several proteins that are differentially accumulated between AD and NDC individuals. Most of them have been reported to be modified in the GM, particularly in the vicinity of AP and NFT. The absence of such lesions in PVWM implies that direct proximity is not necessary to induce changes in this group of proteins, which may represent a non-specific and pervasive reaction to several factors such as oligemia, chronic inflammation and oxidative stress that also affect WMP. It has been postulated that loss of proper blood supply to the PVWM is the major cause of "leukoariosis', since these watershed areas are irrigated by the terminal branches of the deep perforating arteries (reviewed by Brown and Thore (2011)). Moreover, in previous studies from our laboratory, we evaluated the WM circulation pathology in AD (Roher et al., 2003b; Kalback et al., 2004; Hunter et al., 2012). Our data suggest that increased vascular amyloid deposits in cortical vessels apparently block the periarterial spaces inducing stagnation of interstitial fluid leading to dilation of the periarterial spaces and edema in the white matter (etat criblé). Furthermore, the number of blood vessels in the areas of rarefaction are significantly decreased which suggest severe white matter hypoperfusion.

5. Conclusions

In summary, the present study attempts to comprehensively assess the morphological and biochemical substrates that underlie WMP in AD. Overall, the proteomic data suggest that a series of proteins involved in the maintenance of the neuronal and glial cytoskeletons, calcium binding proteins and cellular survival are profoundly altered in the PVWM. Immunocytochemical and electron microscopy analyses of WMR areas clearly reveals an extensive demise of axons and myelin with concomitant enlargement of astroglial processes partially infiltrating the vacuum left by the loss of myelinated axons which amount to as much as 30%.

The rapidly accumulating data suggest the intriguing possibility that sustained WM ischemia/hypoxia generates an environment of energy depletion profoundly deranging the normal levels of multiple proteins to trigger a series of devastating biochemical and morphological cascades underlying AD pathogenesis.

Our experiments suggest the provocative hypothesis that not only is WM dysfunction a consequence of AD, but that the magnitude of these lesions may be a precipitating factor in both dementia emergence and evolution. Elucidating the nature of these WM molecular changes will permit a better understanding of AD dementia and define new targets for therapeutic assessment and intervention.

Supplementary Material

Refer to Web version on PubMed Central for supplementary material.

Acknowledgments

This study was supported by the National Institute on Aging grant R01 AG019795. The Brain Donation Program at Banner Sun Health Research Institute is supported by the National Institute of Neurological Disorders and Stroke (U24 NS072026) and by The National Institute on Aging (P30 AG19610 Arizona Alzheimer's Disease Core Center), the Arizona Department of Health Services (contract 211002, Arizona Alzheimer's Research Center), the Arizona Biomedical Research Commission (contracts 4001, 0011, 05-901 and 1001 to the Arizona Parkinson's

Disease Consortium) and the Michael J. Fox Foundation for Parkinson's Research. The funders had no role in study design, data collection and analysis, decision to publish or preparation of the manuscript.

Abbreviations

2D-DIGE	2-dimensional difference gel electrophoresis
AD	Alzheimer's disease
ANXA1	annexin A1
AP	amyloid plaques
ApoE	apolipoprotein E
CAA	cerebral amyloid angiopathy
CALM	calmodulin
CRMP-2	collapsin response mediator protein-2
DTI	diffusion tenor imaging
FSCN1	fascin 1
GFAP	glial fibrillary acidic protein
GM	gray matter
H&E	hematoxylin and eosin
INA	α-internexin
MCI	mild cognitive impairment
MRI	magnetic resonance imaging
NDC	non-demented control
NFT	neurofibrillary tangles
OD	optical density
PBS	phosphate buffered saline
PBS-T	phosphate buffered saline containing 0.3% Tween20
PVWM	periventricular white matter
RT	room temperature
TFA	trifluoroacetic acid
TMS	thymosine
TPM	tropomyosin
WM	white matter
WMH	white matter hyperintensities
WMP	white matter pathology
WMR	white matter rarefaction
VDAC1	voltage-dependent anion channel 1
VIM	vimentin

Reference List

Adams JC. Roles of fascin in cell adhesion and motility. Curr. Opin. Cell Biol. 2004; 16:590–596. [PubMed: 15363811]

Al-Hasani OH, Smith C. Traumatic white matter injury and toxic leukoencephalopathies. Expert. Rev. Neurother. 2011; 11:1315–1324. [PubMed: 21864077]

Arimura N, Menager C, Kawano Y, Yoshimura T, Kawabata S, Hattori A, Fukata Y, Amano M, Goshima Y, Inagaki M, Morone N, Usukura J, Kaibuchi K. Phosphorylation by Rho kinase regulates CRMP-2 activity in growth cones. Mol. Cell Biol. 2005; 25:9973–9984. [PubMed: 16260611]

Arumugam T, Simeone DM, Schmidt AM, Logsdon CD. S100P stimulates cell proliferation and survival via receptor for activated glycation end products (RAGE). J. Biol. Chem. 2004; 279:5059–5065. [PubMed: 14617629]

Bartzokis G. Age-related myelin breakdown: a developmental model of cognitive decline and Alzheimer's disease. Neurobiol. Aging. 2004; 25:5–18. [PubMed: 14675724]

Bartzokis G. Alzheimer's disease as homeostatic responses to age-related myelin breakdown. Neurobiol. Aging. 2011; 32:1341–1371. [PubMed: 19775776]

Beach TG, Sue LI, Walker DG, Roher AE, Lue L, Vedders L, Connor DJ, Sabbagh MN, Rogers J. The Sun Health Research Institute Brain Donation Program: description and experience, 1987-2007. Cell Tissue Bank. 2008; 9:229–245. [PubMed: 18347928]

Beach TG, Walker R, McGeer EG. Patterns of gliosis in Alzheimer's disease and aging cerebrum. Glia. 1989; 2:420–436. [PubMed: 2531723]

Beaulieu C. The basis of anisotropic water diffusion in the nervous system - a technical review. NMR Biomed. 2002; 15:435–455. [PubMed: 12489094]

Bozzali M, Falini A, Franceschi M, Cercignani M, Zuffi M, Scotti G, Comi G, Filippi M. White matter damage in Alzheimer's disease assessed in vivo using diffusion tensor magnetic resonance imaging. J. Neurol. Neurosurg. Psychiatry. 2002; 72:742–746. [PubMed: 12023417]

Braak H, Braak E. Development of Alzheimer-related neurofibrillary changes in the neocortex inversely recapitulates cortical myelogenesis. Acta Neuropathol. 1996; 92:197–201. [PubMed: 8841666]

Braak H, Del Tredici K. Poor and protracted myelination as a contributory factor to neurodegenerative disorders. Neurobiol. Aging. 2004; 25:19–23. [PubMed: 14675725]

Bronge L, Bogdanovic N, Wahlund LO. Postmortem MRI and histopathology of white matter changes in Alzheimer brains. A quantitative, comparative study. Dement. Geriatr. Cogn Disord. 2002; 13:205–212. [PubMed: 12006730]

Brown WR, Thore CR. Review: cerebral microvascular pathology in ageing and neurodegeneration. Neuropathol. Appl. Neurobiol. 2011; 37:56–74. [PubMed: 20946471]

Brun A, Englund E. A white matter disorder in dementia of the Alzheimer type: a pathoanatomical study. Ann. Neurol. 1986; 19:253–262. [PubMed: 3963770]

Brunetti A, Postiglione A, Tedeschi E, Ciarmiello A, Quarantelli M, Covelli EM, Milan G, Larobina M, Soricelli A, Sodano A, Alfano B. Measurement of global brain atrophy in Alzheimer's disease with unsupervised segmentation of spin-echo MRI studies. J. Magn Reson. Imaging. 2000; 11:260–266. [PubMed: 10739557]

Chin D, Means AR. Calmodulin: a prototypical calcium sensor. Trends Cell Biol. 2000; 10:322–328. [PubMed: 10884684]

Choi SJ, Lim KO, Monteiro I, Reisberg B. Diffusion tensor imaging of frontal white matter microstructure in early Alzheimer's disease: a preliminary study. J. Geriatr. Psychiatry Neurol. 2005; 18:12–19. [PubMed: 15681623]

Crockford D, Turjman N, Allan C, Angel J. Thymosin beta4: structure, function, and biological properties supporting current and future clinical applications. Ann. N. Y. Acad. Sci. 2010; 1194:179–189. [PubMed: 20536467]

Dawson MR, Polito A, Levine JM, Reynolds R. NG2-expressing glial progenitor cells: an abundant and widespread population of cycling cells in the adult rat CNS. Mol. Cell Neurosci. 2003; 24:476–488. [PubMed: 14572468]

DeCarli C, Grady CL, Clark CM, Katz DA, Brady DR, Murphy DG, Haxby JV, Salerno JA, Gillette JA, Gonzalez-Aviles A, Rapoport SI. Comparison of positron emission tomography, cognition, and brain volume in Alzheimer's disease with and without severe abnormalities of white matter. J. Neurol. Neurosurg. Psychiatry. 1996; 60:158–167. [PubMed: 8708645]

Delacourte A. General and dramatic glial reaction in Alzheimer brains. Neurology. 1990; 40:33–37. [PubMed: 2296379]

Duan JH, Wang HQ, Xu J, Lin X, Chen SQ, Kang Z, Yao ZB. White matter damage of patients with Alzheimer's disease correlated with the decreased cognitive function. Surg. Radiol. Anat. 2006; 28:150–156. [PubMed: 16614789]

Duffy PE, Rapport M, Graf L. Glial fibrillary acidic protein and Alzheimer-type senile dementia. Neurology. 1980; 30:778–782. [PubMed: 7190246]

Ecroyd H, Carver JA. Crystallin proteins and amyloid fibrils. Cell Mol. Life Sci. 2009; 66:62–81. [PubMed: 18810322]

Englund E, Brun A. White matter changes in dementia of Alzheimer's type: the difference in vulnerability between cell compartments. Histopathology. 1990; 16:433–439. [PubMed: 2361659]

Ewing RM, Chu P, Elisma F, Li H, Taylor P, Climie S, Broom-Cerajewski L, Robinson MD, O'Connor L, Li M, Taylor R, Dharsee M, Ho Y, Heilbut A, Moore L, Zhang S, Ornatsky O, Bukhman YV, Ethier M, Sheng Y, Vasilescu J, Abu-Farha M, Lambert JP, Duewel HS, Stewart II, Kuehl B, Hogue K, Colwill K, Gladwish K, Muskat B, Kinach R, Adams SL, Moran MF, Morin GB, Topaloglou T, Figeys D. Large-scale mapping of human protein-protein interactions by mass spectrometry. Mol. Syst. Biol. 2007; 3:89. [PubMed: 17353931]

Fath T, Fischer RS, Dehmelt L, Halpain S, Fowler VM. Tropomodulins are negative regulators of neurite outgrowth. Eur. J. Cell Biol. 2011; 90:291–300. [PubMed: 21146252]

Faye C, Chautard E, Olsen BR, Ricard-Blum S. The first draft of the endostatin interaction network. J. Biol. Chem. 2009; 284:22041–22047. [PubMed: 19542224]

Fellgiebel A, Muller MJ, Wille P, Dellani PR, Scheurich A, Schmidt LG, Stoeter P. Color-coded diffusion-tensor-imaging of posterior cingulate fiber tracts in mild cognitive impairment. Neurobiol. Aging. 2005; 26:1193–1198. [PubMed: 15917103]

Fernandez-Gamba A, Leal MC, Maarouf CL, Richter-Landsberg C, Wu T, Morelli L, Roher AE, Castano EM. Collapsin response mediator protein-2 phosphorylation promotes the reversible retraction of oligodendrocyte processes in response to non-lethal oxidative stress. J. Neurochem. 2012; 121:985–995. [PubMed: 22443207]

Gong B, Cao Z, Zheng P, Vitolo OV, Liu S, Staniszewski A, Moolman D, Zhang H, Shelanski M, Arancio O. Ubiquitin hydrolase Uch-L1 rescues beta-amyloid-induced decreases in synaptic function and contextual memory. Cell. 2006; 126:775–788. [PubMed: 16923396]

Gouw AA, Seewann A, Vrenken H, van Der Flier WM, Rozemuller JM, Barkhof F, Scheltens P, Geurts JJ. Heterogeneity of white matter hyperintensities in Alzheimer's disease: post-mortem quantitative MRI and neuropathology. Brain. 2008; 131:3286–3298. [PubMed: 18927145]

Hachinski VC, Potter P, Merskey H. Leuko-araiosis. Arch. Neurol. 1987; 44:21–23. [PubMed: 3800716]

Hagemann TL, Boelens WC, Wawrousek EF, Messing A. Suppression of GFAP toxicity by alphaB-crystallin in mouse models of Alexander disease. Hum. Mol. Genet. 2009; 18:1190–1199. [PubMed: 19129171]

Hannappel E. Thymosin beta4 and its posttranslational modifications. Ann. N. Y. Acad. Sci. 2010; 1194:27–35. [PubMed: 20536447]

Hunter JM, Kwan J, Malek-Ahmadi M, Maarouf CL, Kokjohn TA, Belden C, Sabbagh MN, Beach TG, Roher AE. Morphological and pathological evolution of the brain microcirculation in aging and Alzheimer's disease. PLoS. One. 2012; 7:e36893. [PubMed: 22615835]

Jana M, Palencia CA, Pahan K. Fibrillar amyloid-beta peptides activate microglia via TLR2: implications for Alzheimer's disease. J. Immunol. 2008; 181:7254–7262. [PubMed: 18981147]

Jesse S, Steinacker P, Cepek L, von Arnim CA, Tumani H, Lehnert S, Kretzschmar HA, Baier M, Otto M. Glial fibrillary acidic protein and protein S-100B: different concentration pattern of glial proteins in cerebrospinal fluid of patients with Alzheimer's disease and Creutzfeldt-Jakob disease. J. Alzheimers. Dis. 2009; 17:541–551. [PubMed: 19433893]

Kalaria RN. Small vessel disease and Alzheimer's dementia: pathological considerations. Cerebrovasc. Dis. 2002; 13(Suppl 2):48–52. [PubMed: 11901243]

Kalback W, Esh C, Castano EM, Rahman A, Kokjohn T, Luehrs DC, Sue L, Cisneros R, Gerber F, Richardson C, Bohrmann B, Walker DG, Beach TG, Roher AE. Atherosclerosis, vascular amyloidosis and brain hypoperfusion in the pathogenesis of sporadic Alzheimer's disease. Neurol. Res. 2004; 26:525–539. [PubMed: 15265270]

Kashon ML, Ross GW, O'Callaghan JP, Miller DB, Petrovitch H, Burchfiel CM, Sharp DS, Markesbery WR, Davis DG, Hardman J, Nelson J, White LR. Associations of cortical astrogliosis with cognitive performance and dementia status. J. Alzheimers Dis. 2004; 6:595–604. [PubMed: 15665400]

Kawamura J, Meyer JS, Terayama Y, Weathers S. Leuko-araiosis and cerebral hypoperfusion compared in elderly normals and Alzheimer's dementia. J. Am. Geriatr. Soc. 1992; 40:375–380. [PubMed: 1556365]

Korolainen MA, Auriola S, Nyman TA, Alafuzoff I, Pirttila T. Proteomic analysis of glial fibrillary acidic protein in Alzheimer's disease and aging brain. Neurobiol. Dis. 2005; 20:858–870. [PubMed: 15979880]

Larson ME, Sherman MA, Greimel S, Kuskowski M, Schneider JA, Bennett DA, Lesne SE. Soluble alpha-Synuclein Is a Novel Modulator of Alzheimer's Disease Pathophysiology. J. Neurosci. 2012; 32:10253–10266. [PubMed: 22836259]

Linke T, Ross AC, Harrison EH. Proteomic analysis of rat plasma by two-dimensional liquid chromatography and matrix-assisted laser desorption ionization time-of-flight mass spectrometry. J. Chromatogr. A. 2006; 1123:160–169. [PubMed: 16472533]

Maarouf CL, Daugs ID, Kokjohn TA, Walker DG, Hunter JM, Kruchowsky JC, Woltjer R, Kaye J, Castano EM, Sabbagh MN, Beach TG, Roher AE. Alzheimer's disease and non-demented high pathology control nonagenarians: comparing and contrasting the biochemistry of cognitively successful aging. PLoS. One. 2011; 6:e27291. [PubMed: 22087282]

Mancardi GL, Liwnicz BH, Mandybur TI. Fibrous astrocytes in Alzheimer's disease and senile dementia of Alzheimer's type. Acta Neuropathol. 1983; 61:76–80. [PubMed: 6353837]

Medina DA, Gaviria M. Diffusion tensor imaging investigations in Alzheimer's disease: the resurgence of white matter compromise in the cortical dysfunction of the aging brain. Neuropsychiatr. Dis. Treat. 2008; 4:737–742. [PubMed: 19043518]

Muramori F, Kobayashi K, Nakamura I. A quantitative study of neurofibrillary tangles, senile plaques and astrocytes in the hippocampal subdivisions and entorhinal cortex in Alzheimer's disease, normal controls and non-Alzheimer neuropsychiatric diseases. Psychiatry Clin. Neurosci. 1998; 52:593–599. [PubMed: 9895207]

National Institute on Aging. Consensus recommendations for the postmortem diagnosis of Alzheimer's disease. The National Institute on Aging, and Reagan Institute Working Group on Diagnostic Criteria for the Neuropathological Assessment of Alzheimer's Disease. Neurobiol. Aging. 18:S1–S2.

Nielsen AL, Holm IE, Johansen M, Bonven B, Jorgensen P, Jorgensen AL. A new splice variant of glial fibrillary acidic protein, GFAP epsilon, interacts with the presenilin proteins. J. Biol. Chem. 2002; 277:29983–29991. [PubMed: 12058025]

O'Dwyer L, Lamberton F, Bokde AL, Ewers M, Faluyi YO, Tanner C, Mazoyer B, O'Neill D, Bartley M, Collins DR, Coughlan T, Prvulovic D, Hampel H. Multiple indices of diffusion identifies white matter damage in mild cognitive impairment and Alzheimer's disease. PLoS. One. 2011a; 6:e21745. [PubMed: 21738785]

O'Dwyer L, Lamberton F, Bokde AL, Ewers M, Faluyi YO, Tanner C, Mazoyer B, O'Neill D, Bartley M, Collins DR, Coughlan T, Prvulovic D, Hampel H. Using diffusion tensor imaging and mixed-effects models to investigate primary and secondary white matter degeneration in Alzheimer's disease and mild cognitive impairment. J. Alzheimers. Dis. 2011b; 26:667–682. [PubMed: 21694456]

Owen JB, Di DF, Sultana R, Perluigi M, Cini C, Pierce WM, Butterfield DA. Proteomi cs-determined differences in the concanavalin-A-fractionated proteome of hippocampus and inferior parietal lobule in subjects with Alzheimer's disease and mild cognitive impairment: implications for progression of AD. J. Proteome. Res. 2009; 8:471–482. [PubMed: 19072283]

Petito CK, Morgello S, Felix JC, Lesser ML. The two patterns of reactive astrocytosis in postischemic rat brain. J. Cereb. Blood Flow Metab. 1990; 10:850–859. [PubMed: 2211878]

Pierpaoli C, Basser PJ. Toward a quantitative assessment of diffusion anisotropy. Magn Reson. Med. 1996; 36:893–906. [PubMed: 8946355]

Polvikoski TM, van Straaten EC, Barkhof F, Sulkava R, Aronen HJ, Niinisto L, Oinas M, Scheltens P, Erkinjuntti T, Kalaria RN. Frontal lobe white matter hyperintensities and neurofibrillary pathology in the oldest old. Neurology. 2010; 75:2071–2078. [PubMed: 21048201]

Reisberg, B.; Pattschull-Furlan, A.; Franssen, E.; Sclan, SG.; Kluger, A.; Dingcong, L.; Ferris, SH. Dementia of the Alzheimer type recapitulates ontogeny inversely on specific ordinal and temporal parameters. In: Kostovic, I.; Knezevic, S.; Wisniewski, HM.; Spillich, GJ., editors. Neurodevelopment, aging and cognition. Birkhäuser; Boston: 1992. p. 345-369.

Roher AE, Esh C, Kokjohn TA, Kalback W, Luehrs DC, Seward JD, Sue LI, Beach TG. Circle of Willis atherosclerosis is a risk factor for sporadic Alzheimer's disease. Arterioscler. Thromb. Vasc. Biol. 2003a; 23:2055–2062. [PubMed: 14512367]

Roher AE, Kuo YM, Esh C, Knebel C, Weiss N, Kalback W, Luehrs DC, Childress JL, Beach TG, Weller RO, Kokjohn TA. Cortical and leptomeningeal cerebrovascular amyloid and white matter pathology in Alzheimer's disease. Mol. Med. 2003b; 9:112–122. [PubMed: 12865947]

Roher AE, Weiss N, Kokjohn TA, Kuo YM, Kalback W, Anthony J, Watson D, Luehrs DC, Sue L, Walker D, Emmerling M, Goux W, Beach T. Increased A beta peptides and reduced cholesterol and myelin proteins characterize white matter degeneration in Alzheimer's disease. Biochemistry. 2002; 41:11080–11090. [PubMed: 12220172]

Rose SE, McMahon KL, Janke AL, O'Dowd B, de Zubicaray G, Strudwick MW, Chalk JB. Diffusion indices on magnetic resonance imaging and neuropsychological performance in amnestic mild cognitive impairment. J. Neurol. Neurosurg. Psychiatry. 2006; 77:1122–1128. [PubMed: 16754694]

Ruelle V, Falisse-Poirrier N, Elmoualij B, Zorzi D, Pierard O, Heinen E, De Pauw E, Zorzi W. An immuno-PF2D-MS/MS proteomic approach for bacterial antigenic characterization: to Bacillus and beyond. J. Proteome. Res. 2007; 6:2168–2175. [PubMed: 17488104]

Salat DH, Tuch DS, van der Kouwe AJ, Greve DN, Pappu V, Lee SY, Hevelone ND, Zaleta AK, Growdon JH, Corkin S, Fischl B, Rosas HD. White matter pathology isolates the hippocampal formation in Alzheimer's disease. Neurobiol. Aging. 2010; 31:244–256. [PubMed: 18455835]

Schechter R, Yen SH, Terry RD. Fibrous Astrocytes in senile dementia of the Alzheimer type. J. Neuropathol. Exp. Neurol. 1981; 40:95–101. [PubMed: 7007585]

Scheltens P, Barkhof F, Leys D, Wolters EC, Ravid R, Kamphorst W. Histopathologic correlates of white matter changes on MRI in Alzheimer's disease and normal aging. Neurology. 1995; 45:883–888. [PubMed: 7746401]

Schevzov G, Bryce NS, monte-Baldonado R, Joya J, Lin JJ, Hardeman E, Weinberger R, Gunning P. Specific features of neuronal size and shape are regulated by tropomyosin isoforms. Mol. Biol. Cell. 2005; 16:3425–3437. [PubMed: 15888546]

Selden NR, Gitelman DR, Salamon-Murayama N, Parrish TB, Mesulam MM. Trajectories of cholinergic pathways within the cerebral hemispheres of the human brain. Brain. 1998; 121(Pt 12): 2249–2257. [PubMed: 9874478]

Sjobeck M, Haglund M, Englund E. White matter mapping in Alzheimer's disease: A neuropathological study. Neurobiol. Aging. 2006; 27:673–680. [PubMed: 15894407]

Smith CD, Snowdon DA, Wang H, Markesbery WR. White matter volumes and periventricular white matter hyperintensities in aging and dementia. Neurology. 2000; 54:838–842. [PubMed: 10690973]

Smith RC, Rosen KM, Pola R, Magrane J. Stress proteins in Alzheimer's disease. Int. J. Hyperthermia. 2005; 21:421–431. [PubMed: 16048839]

Sofroniew MV. Molecular dissection of reactive astrogliosis and glial scar formation. Trends Neurosci. 2009; 32:638–647. [PubMed: 19782411]

Stricker NH, Schweinsburg BC, Delano-Wood L, Wierenga CE, Bangen KJ, Haaland KY, Frank LR, Salmon DP, Bondi MW. Decreased white matter integrity in late-myelinating fiber pathways in Alzheimer's disease supports retrogenesis. Neuroimage. 2009; 45:10–16. [PubMed: 19100839]

Suter OC, Sunthorn T, Kraftsik R, Straubel J, Darekar P, Khalili K, Miklossy J. Cerebral hypoperfusion generates cortical watershed microinfarcts in Alzheimer disease. Stroke. 2002; 33:1986–1992. [PubMed: 12154250]

Tang G, Perng MD, Wilk S, Quinlan R, Goldman JE. Oligomers of mutant glial fibrillary acidic protein (GFAP) Inhibit the proteasome system in alexander disease astrocytes, and the small heat shock protein alphaB-crystallin reverses the inhibition. J. Biol. Chem. 2010; 285:10527–10537. [PubMed: 20110364]

Toyooka T, Nawashiro H, Shinomiya N, Shima K. Down-regulation of glial fibrillary acidic protein and vimentin by RNA interference improves acute urinary dysfunction associated with spinal cord injury in rats. J. Neurotrauma. 2011; 28:607–618. [PubMed: 21250919]

Uchida Y, Ohshima T, Sasaki Y, Suzuki H, Yanai S, Yamashita N, Nakamura F, Takei K, Ihara Y, Mikoshiba K, Kolattukudy P, Honnorat J, Goshima Y. Semaphorin3A signalling is mediated via sequential Cdk5 and GSK3beta phosphorylation of CRMP2: implication of common phosphorylating mechanism underlying axon guidance and Alzheimer's disease. Genes Cells. 2005; 10:165–179. [PubMed: 15676027]

van Straaten EC, Harvey D, Scheltens P, Barkhof F, Petersen RC, Thal LJ, Jack CR Jr. DeCarli C. Periventricular white matter hyperintensities increase the likelihood of progression from amnestic mild cognitive impairment to dementia. J. Neurol. 2008; 255:1302–1308. [PubMed: 18825439]

Wallin A, Blennow K, Rosengren LE. Glial fibrillary acidic protein in the cerebrospinal fluid of patients with dementia. Dementia. 1996; 7:267–272. [PubMed: 8872418]

Wang K, Bekar LK, Furber K, Walz W. Vimentin-expressing proximal reactive astrocytes correlate with migration rather than proliferation following focal brain injury. Brain Res. 2004; 1024:193–202. [PubMed: 15451382]

Wilhelmsson U, Li L, Pekna M, Berthold CH, Blom S, Eliasson C, Renner O, Bushong E, Ellisman M, Morgan TE, Pekny M. Absence of glial fibrillary acidic protein and vimentin prevents hypertrophy of astrocytic processes and improves post-traumatic regeneration. J. Neurosci. 2004; 24:5016–5021. [PubMed: 15163694]

Yuan S, Fu Y, Wang X, Shi H, Huang Y, Song X, Li L, Song N, Luo Y. Voltage-dependent anion channel 1 is involved in endostatin-induced endothelial cell apoptosis. FASEB J. 2008; 22:2809–2820. [PubMed: 18381814]

Zhang Y, Schuff N, Du AT, Rosen HJ, Kramer JH, Gorno-Tempini ML, Miller BL, Weiner MW. White matter damage in frontotemporal dementia and Alzheimer's disease measured by diffusion MRI. Brain. 2009; 132:2579–2592. [PubMed: 19439421]

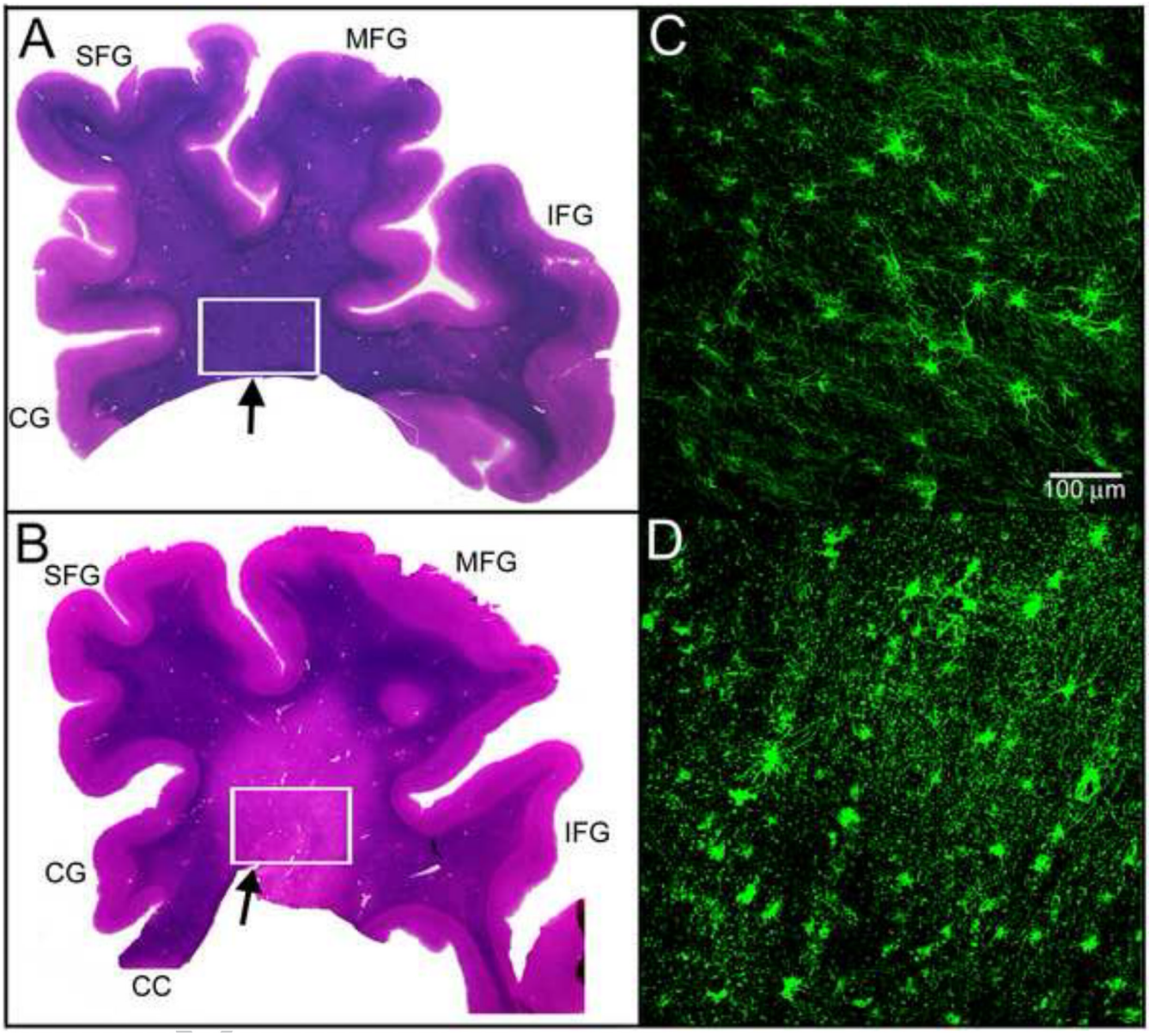

Figure 1.

Coronal sections from the frontal lobe at the level of the genu of the corpus callosum and immunohistological sections of deep WM stained with anti-GFAP/Alexa Fluor 488. **A**) A representative section of a NDC individual (case #4) showing an intense and homogeneous distribution of the H&E stain throughout the WM. **B**) An example of extensive WM rarefaction in AD (case #13). In this section, the apparent pallor of the H&E stain reveals extensive WM loss comprising the periventricular and deep WM. The boxed areas in both cases depict the areas of PVWM tissue used in the proteomic analysis and the arrows designate the superior angle of the anterior horn of the lateral ventricle. **C**) Immunohistological section of the deep WM of NDC case #4 astrocytes. The morphology of the astrocyte shows a stellar body with fine ramified fibrous processes with smooth surfaces that extend over long distances. **D)** Section of the deep WM from AD case #13. Most of the astrocyte bodies resemble the protoplasmic type with shorter processes of variable caliber. There is an extensive distribution of granular positive GFAP that may correspond to dilated

astrocytic cell processes probably filling areas of extensive axonal demise (see Figure 2). Magnification = 200X. Scale bar in (C) also applies to (D). CC, corpus callosum; CG, cingulate gyrus; SFG, superior frontal gyrus; MFG, middle frontal gyrus; IFG, inferior frontal gyrus.

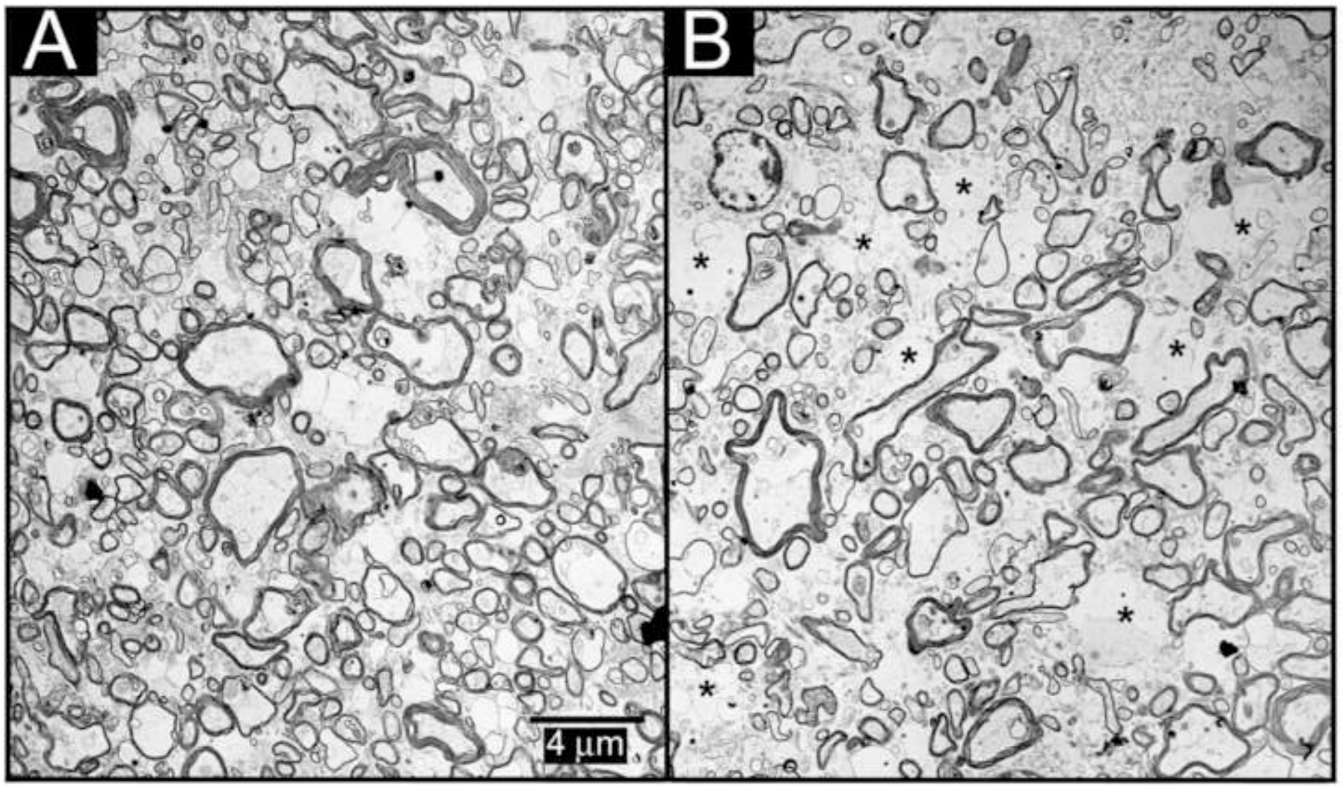

Figure 2.

Electron micrographs of frontal WM. **A**) Electron micrograph section of a 90 year old NDC female, with a total WMR score of 0, showing a homogeneous distribution of axons with different degrees of myelination. **B)** An 87 year old AD female with a total WMR score of 10, demonstrating a severe loss of axons and myelin surrounded by dilated astrocytic processes (designated by asterisks) with a 'watery appearance' that fill the gaps left by axonal downfall that may explain the granular positive GFAP impression shown in Figure 1D. Axonal counting revealed a difference of 30% loss in the AD case relative to the NDC. Magnification = 2000X. Scale bar in (A) applies to (B). The tissues were fixed in the immediate postmortem in 2% paraformaldehyde, 1.25% glutaraldehyde, 0.075% calcium chloride in 0.1 M Na cacodylate buffer pH 7.4. The electron micrographs are a courtesy of Dr. Bernd Bohrmann, Hoffman-La Roche, Basel Switzerland.

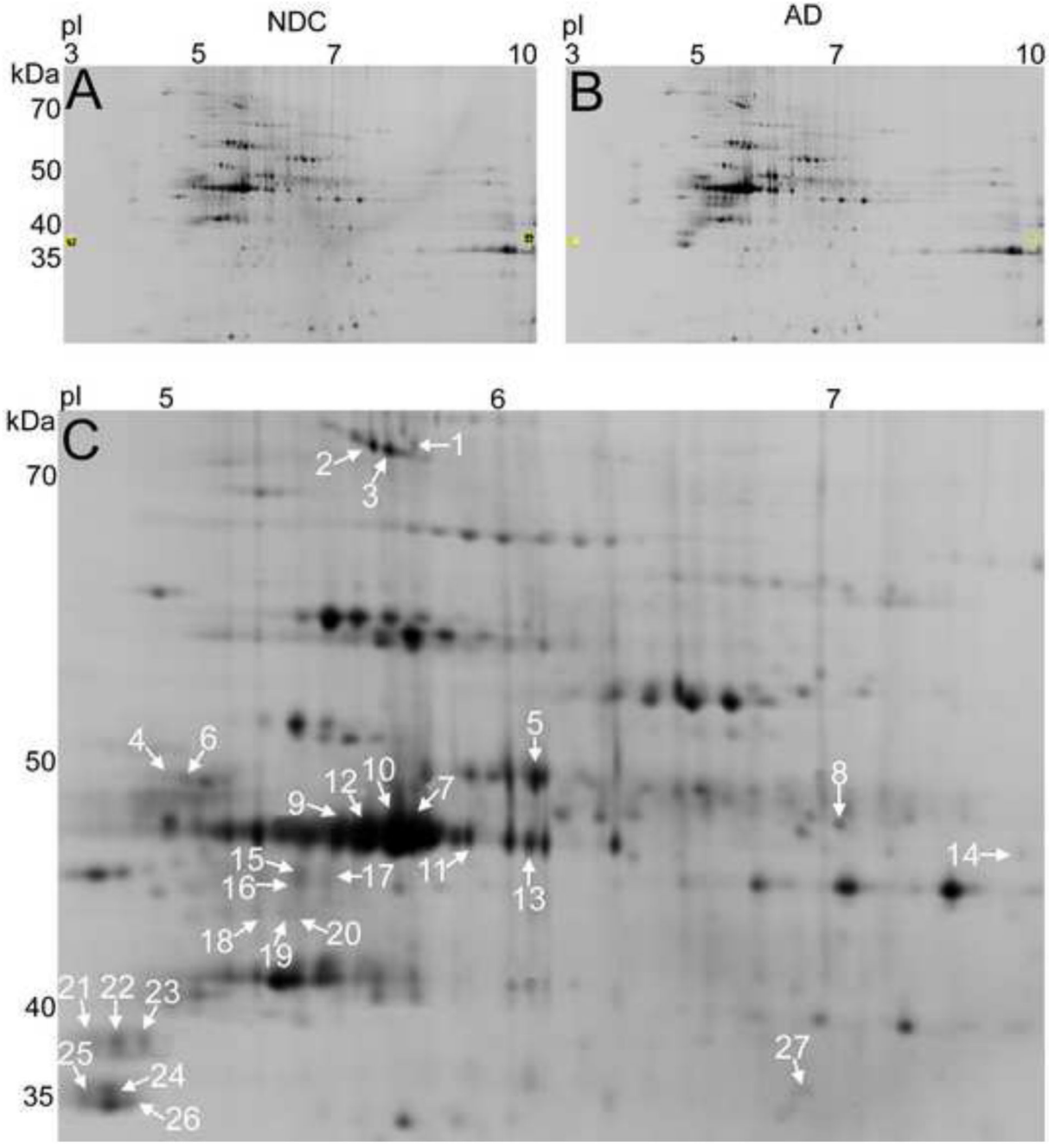

Figure 3.

2D-DIGE analysis of the NDC pool (A) and AD pool (B) of PVWM pellet proteins. C) Zoomed in area of the NDC gel showing identified spots in more detail. The numbers in (C) correspond to Table 2 spot numbers with mass spectrometry protein identifications. Isoelectric points (pI) are given across the top of each gel and molecular weigh in kiloDaltons (kDa) along the left side. Note that pI and molecular weight are approximate.

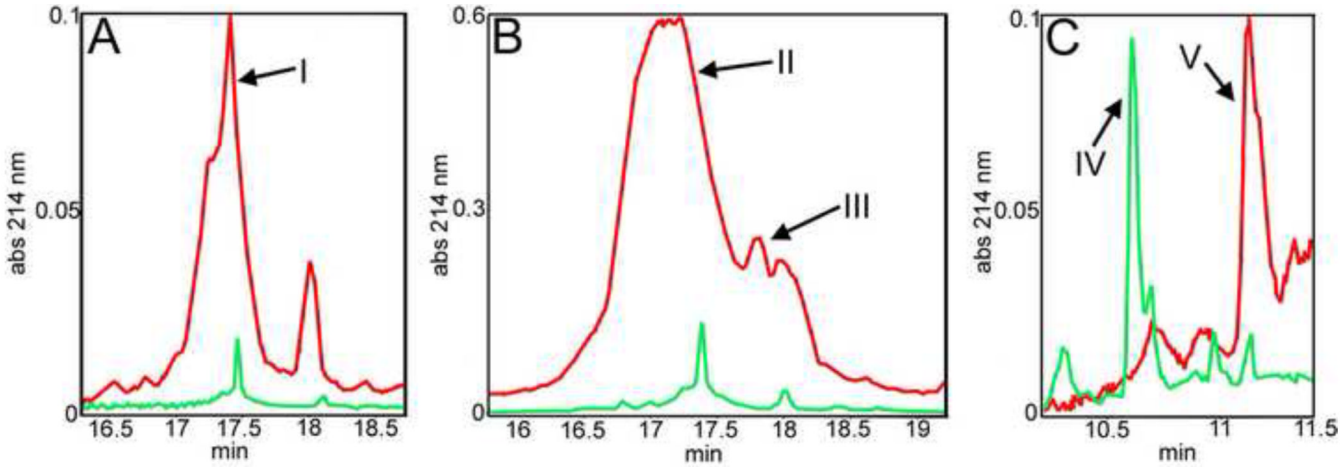

Figure 4.

After fractionation based on pH, AD (red) and NDC (green) PVWM soluble protein pools were separated on a reverse phase column. After filtering the data, 5 fractions were selected for mass spectrometry protein identification. A) Fraction I mass spectrometry results are shown in Table 3. B) Fractions II and III mass spectrometry results are shown in Table 5. C) Fraction IV mass spectrometry results are shown in Table 5 and Fraction V shown in Table 6.

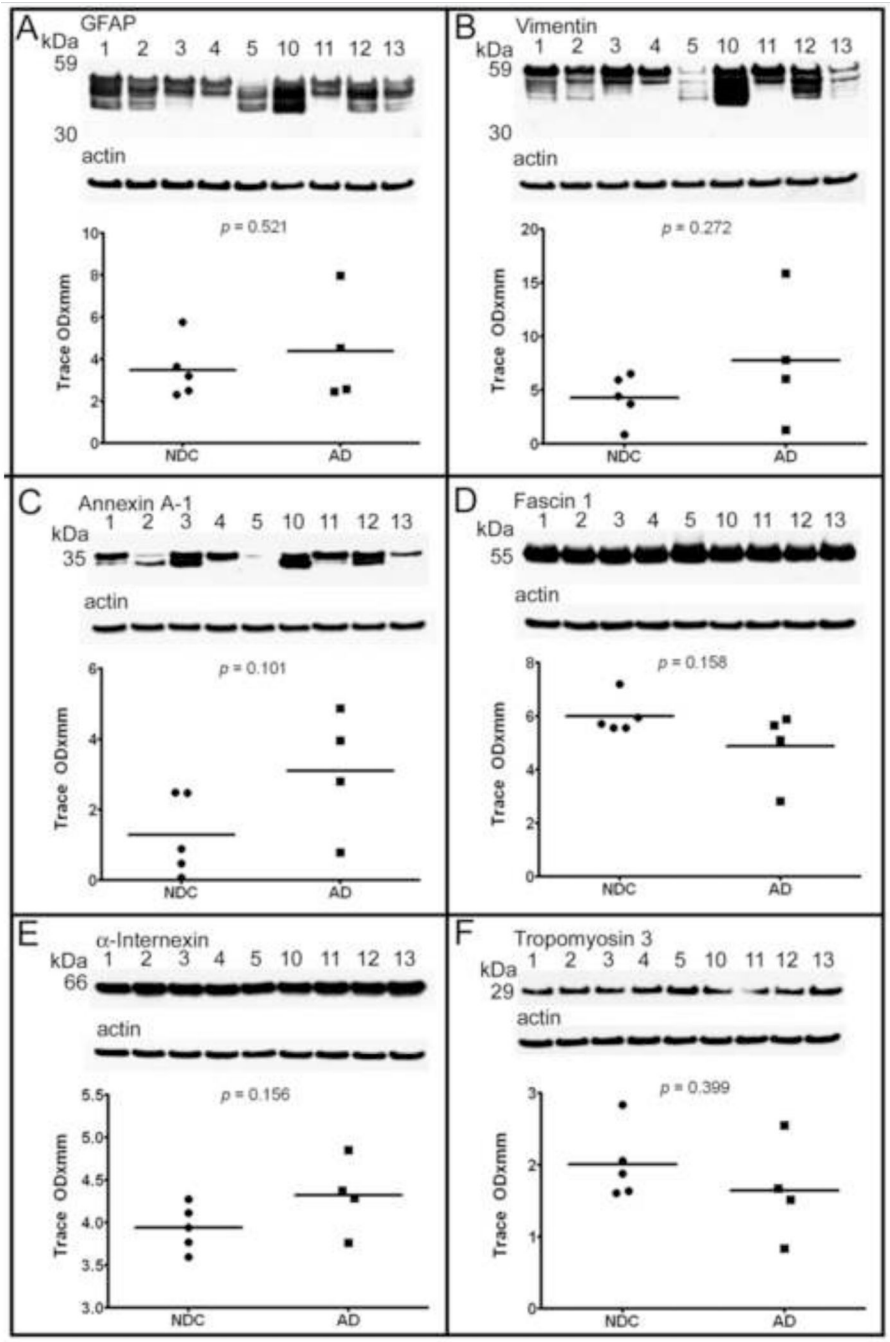

Figure 5.

1D SDS-PAGE Western blots of individual AD and NDC subjects. Antibody details are given in supplementary Table I. Case numbers provided at the top of each blot correspond to those in Table 1: Cases 1-5 = NDC and cases 10-13 = AD. All blots were stripped and re-probed with actin and are provided below each blot. Statistical analysis was performed with an unpaired, 2-tailed, t-test.

Table 1

Study subject demographics and neuropathology assessments

NDC	Expired age (yrs)	Gender	PMI (h)	Brain weight (g)	ApoE GT	Total plaque score	Total NFT score	Braak stage	Total CAA score	Total WMR score
1	85	M	3.2	1280	3/3	0.00	4.25	II	0	0
2	92	M	3.8	1165	3/3	1.33	3.13	III	0	0
3	86	M	3.0	1055	3/3	4.25	1.00	I	0	0
4	82	F	2.3	940	3/3	0.00	3.50	II	0	0
5	87	F	2.0	1120	2/3	5.00	4.50	III	0	0
Mean	86.4		2.8	1112		2.12	3.18		0	0

AD	Expired age (yrs)	Gender	PMI (h)	Brain weight (g)	ApoE GT	Total plaque score	Total NFT score	Braak stage	Total CAA score	Total WMR score
10	87	F	4.0	980	3/3	12.50	14.50	V	2	12
11	85	F	1.5	940	3/3	14.00	15.00	VI	2	12
12	86	F	2.5	1220	3/3	15.00	14.00	V	0	12
13	86	M	2.8	1140	3/3	12.50	10.00	IV	4	12
Mean	86.0		2.7	1070		13.50	13.38		2	12

NDC, non-demented control; AD, Alzheimer's disease; yrs, years; M, male; F, female; PMI, postmortem interval; h, hours; g, grams; ApoE, apolipoprotein E; GT, genotype; NFT, neurofibrillary tangles; CAA, cerebral amyloid angiopathy; WMR, white matter rarefaction

Neurochem Int. Author manuscript; available in PMC 2014 January 01.

Table 2

Mass Spectrometry Results from 2D-DIGE Analysis of PVWM Proteins

Spot #	Uniprot entry code	Protein name	Gene name	Length (aa)	DB search score	% coverage	# of peptides	AD/NDC fold change
1	P14136	GFAP	GFAP	432	733	81	33	2.03
2		GFAP			680	75	28	2.03
3		GFAP			982	87	33	2.09
4	P08670	VIM	VIM	466	653	74	30	2.19
5	P14136	GFAP	GFAP	432	1020	87	34	2.12
6	P08670	VIM	VIM	466	472	74	30	1.79
7	P14136	GFAP	GFAP	432	866	88	32	2.01
8	Q16658	FSCN1	FSCN1	493	163	39	15	-2.18
9	P14136	GFAP	GFAP	432	1050	87	34	2.20
10		GFAP			1060	70	28	2.03
11		GFAP			857	82	32	2.11
12		GFAP			1170	82	32	2.25
13		GFAP			1120	87	34	2.17
14		GFAP			314	68	23	2.02
15		GFAP			852	78	30	2.02
16		GFAP			1000	84	33	2.06
17		GFAP			705	83	31	2.12
18		GFAP			696	80	30	3.30
19		GFAP			713	81	30	3.64
20		GFAP			820	81	30	3.34
21		GFAP			370	61	21	6.06
22		GFAP			192	65	23	8.75
23		GFAP			371	65	23	6.87
24		GFAP			145	55	19	8.11
25		GFAP			810	73	28	7.51
26		GFAP			260	61	22	7.52
27	P04083	ANXA1	ANXA1		184	39	9	2.24

2D-DIGE; 2-dimensional difference gel electrophoresis; PVWM, perventricular white matter; aa, amino acid; DB, database; AD, Alzheimer's disease; NDC, non-demented control; GFAP, glial fibrillary acidic protein; VIM, vimentin; ANXA1, annexin A1

Table 3

Proteins identified in PF2D Fraction I (5.3-fold increased in AD vs NDC)

UniProt Entry code	Protein name	Gene name	Length (aa)	DB search score*	% coverage
P14136	GFAP isoform-α	GFAP	432	2251	77.5
P06753	TPM α-3 chain	TPM3	284	748	52.4
P09493	TPM α-1 chain	TPM1	284	665	41.5
P62158	CALM	CALM	149	299	62.2
Q16352	INA	INA	499	226	15.4
Q16143	β-synuclein	SNBC	134	105	31.3

*DB, DataBase (NCBInr), Search engine: MASCOT, protein score threshold=82; AD, Alzheimer's disease; NDC, non-demented control; GFAP, glial fibrillary acidic protein; TPM, tropomyosin; CALM, calmodulin; INA, α-internexin

Neurochem Int. Author manuscript; available in PMC 2014 January 01.

Table 4

Proteins identified in PF2D Fractions II & III (4 to 5.6-fold increased in AD vs NDC)

UniProt entry code	Protein name	Gene name	Length (aa)	DB search score*	% coverage
P14136	GFAP isoform-α	GFAP	432	3101	92.4
P08670	VIM	VIM	466	1073	68.2
Q16352	INA	INA	499	641	34.1
P06753	TPM α-3 chain	TPM3	284	474	51.6
P62158	CALM	CALM	149	419	71.5
P67936	TPM α-4 chain	TPM4	248	273	33.9
P25815	Protein S100-P	S100P	95	270	84.8
Q16143	β-synuclein	SNCB	134	237	39.6
P37840	α-synuclein	SNCA	140	233	38.5
A6NLJ7	Ubiquitin carboxyl-terminal esterase L1 (predicted)	UCHL1	100	186	29.1

*DB, DataBase (NCBInr), Search engine: MASCOT, protein score threshold=82; AD, Alzheimer's disease; NDC, non-demented control; GFAP, glial fibrillary acidic protein; VIM, vimentin; INA, α-internexin; TPM, tropomyosin; CALM, calmodulin;

Table 5

Proteins identified in PF2D Fraction IV (10-fold increased in NDC vs AD)

UniProt entry code	Protein name	Gene name	Length (aa)	DB search score*	% coverage
P62328	TMS-β4	TMSB4X	44	404	87.2
P14136	GFAP isoform-α	GFAP	432	278	12. 7
Q16555	CRMP-2	CRMP-2	572	134	6.1
P02686	MBP isoform 1	MBP1	304	127	21.2
P02511	α-B-crystallin	CRYAB	175	91	61.1

*DB, DataBase (NCBInr), Search engine: MASCOT, protein score threshold=82; AD, Alzheimer's disease; NDC, non-demented control; TMS, thymosine; GFAP, glial fibrillary acidic protein; CRMP-2, collapsin response mediator protein-2; MBP, myelin basic protein

Table 6

Proteins identified in PF2D Fraction V (5.5-fold increased in AD vs NDC)

UniProt entry code	Protein name	Gene name	Length (aa)	DB search score*	% coverage
P14136	GFAP isoform-α	GFAP	432	521	18.5
P62328	TMS-β4	TMSB4X	44	321	89.2
P63313	TMS-β10	TMSB10	44	157	46. 5

*DB, DataBase (NCBInr), Search engine: MASCOT, protein score threshold=82; AD, Alzheimer's disease; NDC, non-demented control; GFAP, glial fibrillary acidic protein; TMS, thymosine